

Endotoxemia Accelerates Atherosclerosis Through Electrostatic Charge-Mediated Monocyte Adhesion

Citation for published version (APA):

Schumski, A., Ortega-Gómez, A., Wichapong, K., Winter, C., Lemnitzer, P., Viola, J. R., Pinilla-Vera, M., Folco, E., Solis-Mezarino, V., Völker-Albert, M., Maas, S. L., Pan, C., Perez Olivares, L., Winter, J., Hackeng, T., Karlsson, M. C. I., Zeller, T., Imhof, A., Baron, R. M., ... Soehnlein, O. (2021). Endotoxemia Accelerates Atherosclerosis Through Electrostatic Charge-Mediated Monocyte Adhesion. *Circulation*, 143(3), 254-266. <https://doi.org/10.1161/circulationaha.120.046677>

Document status and date:

Published: 19/01/2021

DOI:

[10.1161/circulationaha.120.046677](https://doi.org/10.1161/circulationaha.120.046677)

Document Version:

Publisher's PDF, also known as Version of record

Document license:

Taverne

Please check the document version of this publication:

- A submitted manuscript is the version of the article upon submission and before peer-review. There can be important differences between the submitted version and the official published version of record. People interested in the research are advised to contact the author for the final version of the publication, or visit the DOI to the publisher's website.
- The final author version and the galley proof are versions of the publication after peer review.
- The final published version features the final layout of the paper including the volume, issue and page numbers.

[Link to publication](#)

General rights

Copyright and moral rights for the publications made accessible in the public portal are retained by the authors and/or other copyright owners and it is a condition of accessing publications that users recognise and abide by the legal requirements associated with these rights.

- Users may download and print one copy of any publication from the public portal for the purpose of private study or research.
- You may not further distribute the material or use it for any profit-making activity or commercial gain
- You may freely distribute the URL identifying the publication in the public portal.

If the publication is distributed under the terms of Article 25fa of the Dutch Copyright Act, indicated by the "Taverne" license above, please follow below link for the End User Agreement:

www.umlib.nl/taverne-license

Take down policy

If you believe that this document breaches copyright please contact us at:

repository@maastrichtuniversity.nl

providing details and we will investigate your claim.

Endotoxemia Accelerates Atherosclerosis Through Electrostatic Charge–Mediated Monocyte Adhesion

BACKGROUND: Acute infection is a well-established risk factor of cardiovascular inflammation increasing the risk for a cardiovascular complication within the first weeks after infection. However, the nature of the processes underlying such aggravation remains unclear. Lipopolysaccharide derived from Gram-negative bacteria is a potent activator of circulating immune cells including neutrophils, which foster inflammation through discharge of neutrophil extracellular traps (NETs). Here, we use a model of endotoxemia to link acute infection and subsequent neutrophil activation with acceleration of vascular inflammation

METHODS: Acute infection was mimicked by injection of a single dose of lipopolysaccharide into hypercholesterolemic mice. Atherosclerosis burden was studied by histomorphometric analysis of the aortic root. Arterial myeloid cell adhesion was quantified by intravital microscopy.

RESULTS: Lipopolysaccharide treatment rapidly enhanced atherosclerotic lesion size by expansion of the lesional myeloid cell accumulation. Lipopolysaccharide treatment led to the deposition of NETs along the arterial lumen, and inhibition of NET release annulled lesion expansion during endotoxemia, thus suggesting that NETs regulate myeloid cell recruitment. To study the mechanism of monocyte adhesion to NETs, we used in vitro adhesion assays and biophysical approaches. In these experiments, NET-resident histone H2a attracted monocytes in a receptor-independent, surface charge–dependent fashion. Therapeutic neutralization of histone H2a by antibodies or by in silico designed cyclic peptides enables us to reduce luminal monocyte adhesion and lesion expansion during endotoxemia.

CONCLUSIONS: Our study shows that NET-associated histone H2a mediates charge-dependent monocyte adhesion to NETs and accelerates atherosclerosis during endotoxemia.

Ariane Schumski, MSc
:
Oliver Soehnlein¹, MD,
PhD

The full author list is available on page 264.

Key Words: atherosclerosis
■ extracellular trap ■ histones
■ inflammation ■ neutrophils ■ sepsis

Sources of Funding, see page 264

© 2020 American Heart Association, Inc.

<https://www.ahajournals.org/journal/circ>

Clinical Perspective

What Is New?

- Neutrophils and specifically neutrophil extracellular traps control accelerated atherosclerosis during endotoxemia.
- Neutrophil extracellular trap resident histone H2a heightens arterial monocyte recruitment in endotoxemia in a mechanism involving electrostatic charge interaction.

What Are the Clinical Implications?

- Neutrophil extracellular trap–driven arterial monocyte recruitment is a mechanism operational during endotoxemia.
- Therapeutic neutralization of neutrophil extracellular trap resident cationic molecules including histone H2a by use of antibodies or peptides may protect patients with cardiovascular risk during an acute infection from secondary cardiovascular events.

Atherosclerosis is a lipid-driven chronic inflammation of the arterial vessel wall. In its late stages, atherosclerosis is the underlying pathophysiology of myocardial infarction and stroke and, hence, the leading cause of mortality worldwide. Monocytes and macrophages hold crucial roles throughout all stages of atherosclerosis because they contribute to lipid modification and respond with a pronounced inflammatory response on uptake of modified lipids.¹ With only limited numbers of macrophages residing in large arteries, the majority of monocytic cells needs to be de novo recruited in a process known as the leukocyte recruitment cascade, which is orchestrated by fine-tuned interactions of selectins, chemokines, and integrins and their respective receptors.² In recent years, studies have provided evidence for the contribution of neutrophils to arterial monocyte recruitment. Herein, neutrophils deposit preformed chemoattractants on endothelial cells or activate endothelial cells directly to stimulate monocyte adhesion.^{3–7}

Multiple bacterial and viral pathogens have been associated with atherosclerosis by seroepidemiological studies and identification of the infectious agent in human atherosclerotic tissue. Moreover, there is strong clinical evidence for the acceleration of arterial inflammation by acute infection.⁸ For example, urinary tract infection and bacteremia associate with an increase in the short-term risk of myocardial infarction.^{9,10} The most striking data, however, are available from patients with pneumonia, with the risk of myocardial infarction peaking at the onset of infection; this risk is proportional to the severity of illness.^{11,12} Division of Gram-negative

bacteria or their elimination leads to release of lipopolysaccharide (LPS) into the bloodstream, that is, endotoxemia. Neutrophils are rapidly activated by LPS possibly leading to the release of neutrophil extracellular traps (NETs), a complex structure composed of nuclear chromatin and proteins of nuclear cytoplasmic and granule origin.¹³ Because the proteins reported to attract monocytes are localized within NETs, and because NETs have been detected at the luminal side of large arteries,¹⁴ we here hypothesized that LPS-triggered NET release acts as a link between endotoxemia and heightened vascular inflammation by triggering monocyte recruitment.

METHODS

An expanded methods section can be found in the [Data Supplement](#). The data that support the findings of this study are available from the corresponding author on reasonable request.

Animal Experiments

We surveyed atheroprogession in *Apoe*^{−/−} or *Apoe*^{−/−} *Cx₃cr1*^{GFP} reporter mice on C57Bl/6J background after 4 weeks of high-fat diet (21% fat, Ssniff). Endotoxemia was induced by intraperitoneal injection of LPS (*Escherichia coli*, O111:B4, Sigma Aldrich, 1 mg/kg body weight, intraperitoneally). Control mice received vehicle (phosphate-buffered saline, 100 μL, intraperitoneally). Thereafter, atherosclerotic lesions were analyzed in aortic root sections or cell adhesion was studied by intravital microscopy of the left carotid artery. To assess the effect of NETs, we blocked NET formation with BB CI-amidine (1 mg/kg body weight, Cayman Chemical Company). In additional experiments, mice received antibodies to histone H2a (20 μg/mouse, Biorbyt), its respective immunoglobulin G isotype control (Jackson ImmunoResearch), or a CHIP (cyclic histone 2A interference peptide; 5 mg/kg body weight). All animal experiments were approved by the local ethics committee and performed in accordance with institutional guidelines.

Intravital Microscopy

Leukocyte-endothelial interactions along the carotid artery were analyzed in *Apoe*^{−/−} *Cx₃cr1*^{GFP} reporter mice by intravital microscopy as previously reported.^{3–5} In brief, mice were placed in a supine position, and the right jugular vein was cannulated with a catheter for antibody injection. Intravital microscopy was performed after injection of a phycoerythrin-conjugated antibody to Ly6G (1 μg; clone 1A8; BioLegend) and 4',6-diamidino-2-phenylindol (Thermo Fischer). With the use of an Olympus BX51 microscope equipped with a Hamamatsu 9100-02 EMCCD camera and a 10× saline-immersion objective, movies of 30 s were acquired and analyzed offline. In the carotid artery, 1 field of view was analyzed per mouse. Green fluorescent protein-expressing cells were considered monocytes. For identification of NET-like structures, the original 4',6-diamidino-2-phenylindol image was transformed into a 8-bit grayscale image and subsequently thresholded. Particles in the latter image were quantified and

particles $>80 \text{ px}^2$ and a circularity <0.75 were considered NET-like structures.

Human Samples

All in vitro experiments were performed with peripheral human white blood cells donated from healthy volunteers. Blood sampling was approved by the Klinikum der Universität München ethics board, and participants gave written informed consent.

Plasma samples from previously described institutional review board–approved biorepositories at Brigham and Women's Hospital¹⁵ were analyzed from patients with Gram-negative rod bacteremia or sepsis with cardiovascular risk factors and compared with those from age-matched controls with cardiovascular risk factors.

Statistics

All statistics analysis was performed by using GraphPad Prism 8 software. Outliers have been determined by Grubbs test with $\alpha=0.05$. To test normal distribution, the Shapiro-Wilk test was used. If normality was passed, data were tested by 2-tailed unpaired *t* test or 1-way ANOVA test. The Mann-Whitney *U* test or Kruskal-Wallis test with the Dunn correction was performed when data were not normally distributed. In all the tests, a 95% confidence interval was used with $P<0.05$, which was assumed as a significant difference. All data are represented as mean \pm SEM.

RESULTS

NETs Induce Luminal Myeloid Cell Adhesion in Atherosclerosis During Endotoxemia

To investigate the effect of endotoxemia on myeloid cell recruitment during atheroprogession, *ApoE*^{-/-} mice were fed a high-fat diet for 4 weeks and injected with LPS for 4 hours (Figure 1A). Treatment in this way resulted in the striking expansion of atherosclerotic lesion sizes (Figure 1B). Although plasma cholesterol and triglyceride levels were not affected by treatment in this way, counts of circulating neutrophils and monocytes were depleted (Figure 1A through 1F in the Data Supplement) likely because of margination and extravasation of activated myeloid cells. The number of neutrophils, monocytes, and macrophages recruited to atherosclerotic lesions, and to inflamed aorta, as well, was drastically increased in LPS-treated mice (Figure 1C and 1D, Figure 1G and 1H in the Data Supplement). This notion was confirmed by the use of intravital microscopy of carotid arteries performed in *ApoE*^{-/-}*Cx3cr1*^{eGFP} mice. There, LPS enhanced adhesion of both GFP⁺ monocytes, and of antibody-labeled neutrophils, as well (Figure 1E and 1F).

LPS is known to trigger the release of NETs¹⁶; hence, we hypothesized that, in our experimental setting, NETs may contribute to heightened neutrophil and monocyte recruitment. Intravital microscopy permitted the

visualization of 4',6-diamidino-2-phenylindol–positive structures with a NET-like shape in the lumen of mice receiving LPS (Figure 1G and 1H). In addition, cell-free DNA, and DNA-myeloperoxidase (MPO) complexes, a plasma marker of NETs, as well, are strikingly increased in the plasma of mice with endotoxemia (Figure 1I and 1J in the Data Supplement). Of note, plasma double-stranded DNA correlated with the number of aortic myeloid cells, and with plasma DNA-MPO complexes, as well, suggesting that plasma double-stranded DNA is a valid surrogate marker of NETs predicting aortic cell infiltration (Figure 1K through 1M in the Data Supplement). Last, plasma DNA-MPO complexes correlated with plasma endotoxin levels, indicating that LPS directly induces NET release (Figure 1N in the Data Supplement). To generate a link to the clinical situation, we assessed the amount of plasma circulating cell-free double-stranded DNA, a surrogate marker of NETs, in patients with cardiovascular risk (Table 1 in the Data Supplement) admitted to the hospital with Gram-negative rod bacteremia or sepsis. Here hospitalized patients with confirmed Gram-negative rod bacteremia or sepsis presented with significantly higher DNA levels than hospitalized matched controls exhibiting the same cardiovascular risk profile, but without Gram-negative rod bacteremia or sepsis (Figure 1M in the Data Supplement). Of note, patients with Gram-negative rod bacteremia or sepsis had higher blood neutrophil counts than the respective control group, and circulating neutrophil counts across both groups of patients correlated with plasma double-stranded DNA levels.

To test whether NETs along the arterial lumen would contribute to the atherosclerosis phenotype observed in endotoxemic mice, we treated mice with BB CI-amidine, a potent inhibitor of PADs (protein arginine deiminases) with favorable pharmacokinetics in terms of plasma half-life and EC₅₀. BB CI-amidine delivery in endotoxemic mice drastically reduced cell-free DNA in the plasma (Figure 1I in the Data Supplement), whereas MPO-DNA complexes were not detectable in this group. Intravital imaging confirmed that BB CI-amidine treatment abrogated luminal NET release in response to stimulation with LPS for 4 hours (Figure 1G and 1H). In addition, heightened lesion formation, and lesional accumulation of myeloid cells, as well, in response to LPS was completely abolished (Figure 1B through 1D, Figure 1G and 1H in the Data Supplement). In agreement herewith, BB CI-amidine treatment led to a vast reduction of arterial myeloid cell adhesion (Figure 1E and 1F), suggesting that luminal NETs promote arterial myeloid cell adhesion during endotoxemia.

NETs Promote Monocyte Adhesion Independent of Receptor Signaling

To study how NETs would promote monocyte adhesion, we allowed human classical monocytes, a

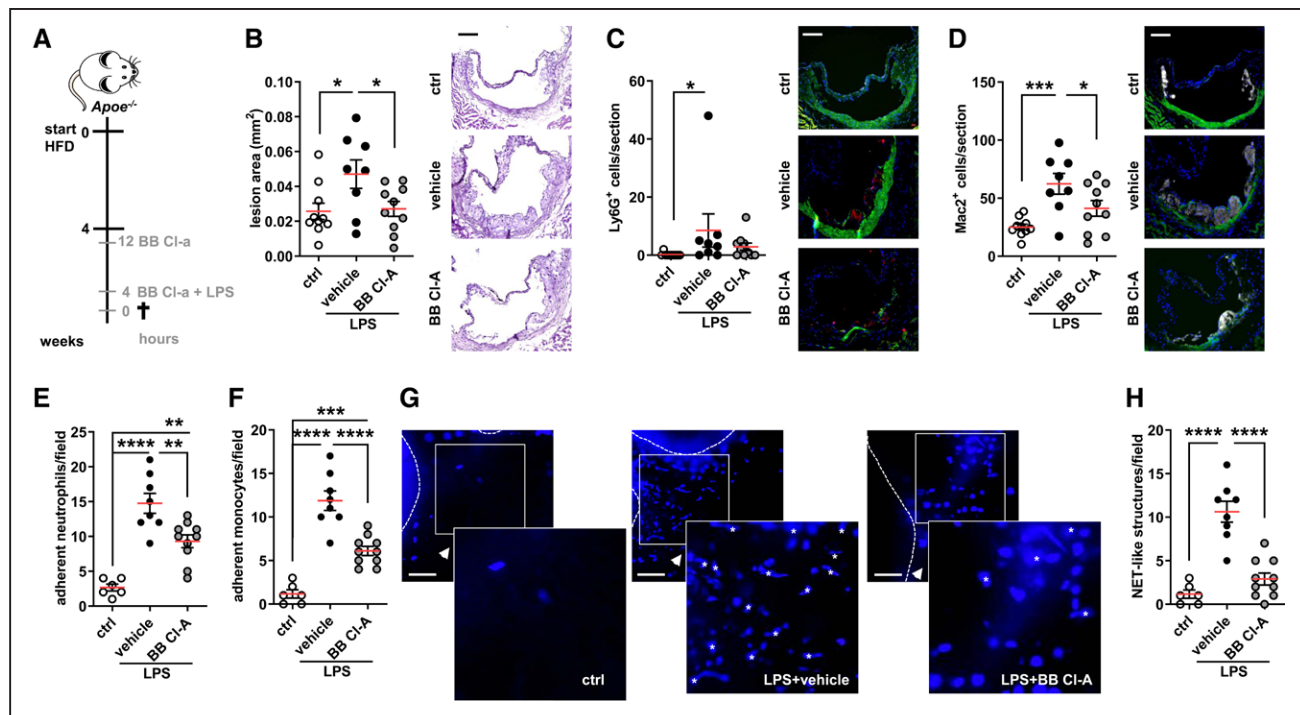


Figure 1. Endotoxemia accelerates atherosclerosis.

A, Experimental setup. *Apoe*^{-/-} or *Apoe*^{-/-}*Cx3cr1*^{flp} mice were fed a HFD for 4 weeks and treated with either phosphate-buffered saline (ctrl) or with LPS (1 mg/kg body weight). Another LPS-treated group received a BB CI-amidine (BB CI-A, 1 mg/kg body weight) 12 hours before and along with LPS injection. **B**, Aortic root lesion size analyzed in hematoxylin and eosin–stained sections. Representative images, scale bar=50 μ m. **C** and **D**, Lesional neutrophils (Ly6G⁺ cells) (**C**) and macrophages (Mac2⁺ cells) (**D**) quantified in root sections. Representative immunofluorescence images showing lesional neutrophil (red), Mac2⁺ positive cells (gray), and nuclei (4',6-diamidino-2-phenylindol, blue), scale bar=50 μ m. **E** and **F**, Quantification of luminally adherent neutrophils (**E**) and monocytes (**F**). **G**, Representative intravital microscopy images of the carotid artery of *Apoe*^{-/-}*Cx3cr1*^{flp} mice. DNA is stained with 4',6-diamidino-2-phenylindol, scale bar 50 μ m. NET-like structures as identified by automatized image analyses are marked up with asterisks. **H**, Count of luminal NET-like structures in left common carotid artery. Data are analyzed by 1-way ANOVA with Tukey multiple comparisons test (**B**, **D**, **E**, **F**, **H**) or Kruskal-Wallis test with Dunn multiple comparisons test (**C**); **P*≤0.05, ***P*≤0.01, ****P*≤0.001, *****P*≤0.0001. All data are presented as mean±SEM. ctrl indicates control; HFD, high-fat diet; LPS, lipopolysaccharide; and NET, neutrophil extracellular trap.

proatherogenic monocyte subset,^{17,18} to sediment on NETs *in vitro*. We witnessed a significant adhesion of monocytes to NET-releasing neutrophils (Figure 2A and 2B). Fluorescence imaging revealed that these classical monocytes predominantly adhered directly to the NET scaffold, and inhibition of monocyte adhesion after NET degradation with DNase I confirmed the importance of NETs in static monocyte adhesion (Figure 2A and 2B). Of note, such a finding could also be recapitulated when using CD4⁺ T cells instead of monocytes (Figure IIA in the Data Supplement). To transfer these findings to a physiologically relevant setting, we initiated NET release in adherent human neutrophils and perfused classical monocytes in a flow chamber assay. As for the static adhesion assay, we found that monocytes primarily bound to DNA fibers and that degradation of NETs abolished adhesion evoked by activated neutrophils (Figure 2C and 2D). Similar data sets were obtained when NETs were induced on tumor necrosis factor–activated endothelial cells. Here, a higher number of classical monocytes was found to adhere at baseline, likely as a consequence of direct monocyte-endothelial cell interaction. The number of adherent monocytes

under static or flow conditions, however, significantly increased when NETs were induced on endothelial cells, an effect fully reversed on DNase I degradation (Figure IIB and IIC in the Data Supplement).

These observations are reminiscent of earlier work showing that proteins typically found in NETs or NETs themselves can increase cell adhesion by engaging chemokine receptor signaling and leukocyte integrin activation.^{2,19–22} Thus, we neutralized chemokine receptors (Figure 2E), receptors of alarmins (Figure 2F, Figure IID in the Data Supplement), or integrins (Figure 2G) before incubation with NETs. Much to our surprise, none of these treatments impacted the adhesion evoked by NETs. Thus, we suspected that the adhesion evoked by NETs may be signaling independent. Depletion of calcium with the use of a chelator did not affect NET-mediated adhesion (Figure IIE in the Data Supplement). In addition, abrogation of signaling of G-protein–coupled receptors by pertussis toxin or even fixation of monocytes with 4% paraformaldehyde did not impair the adhesion of monocytes to NETs (Figure 2H and 2I). Taken together, these data indicate that monocyte adhesion to NETs is independent of receptor signaling.

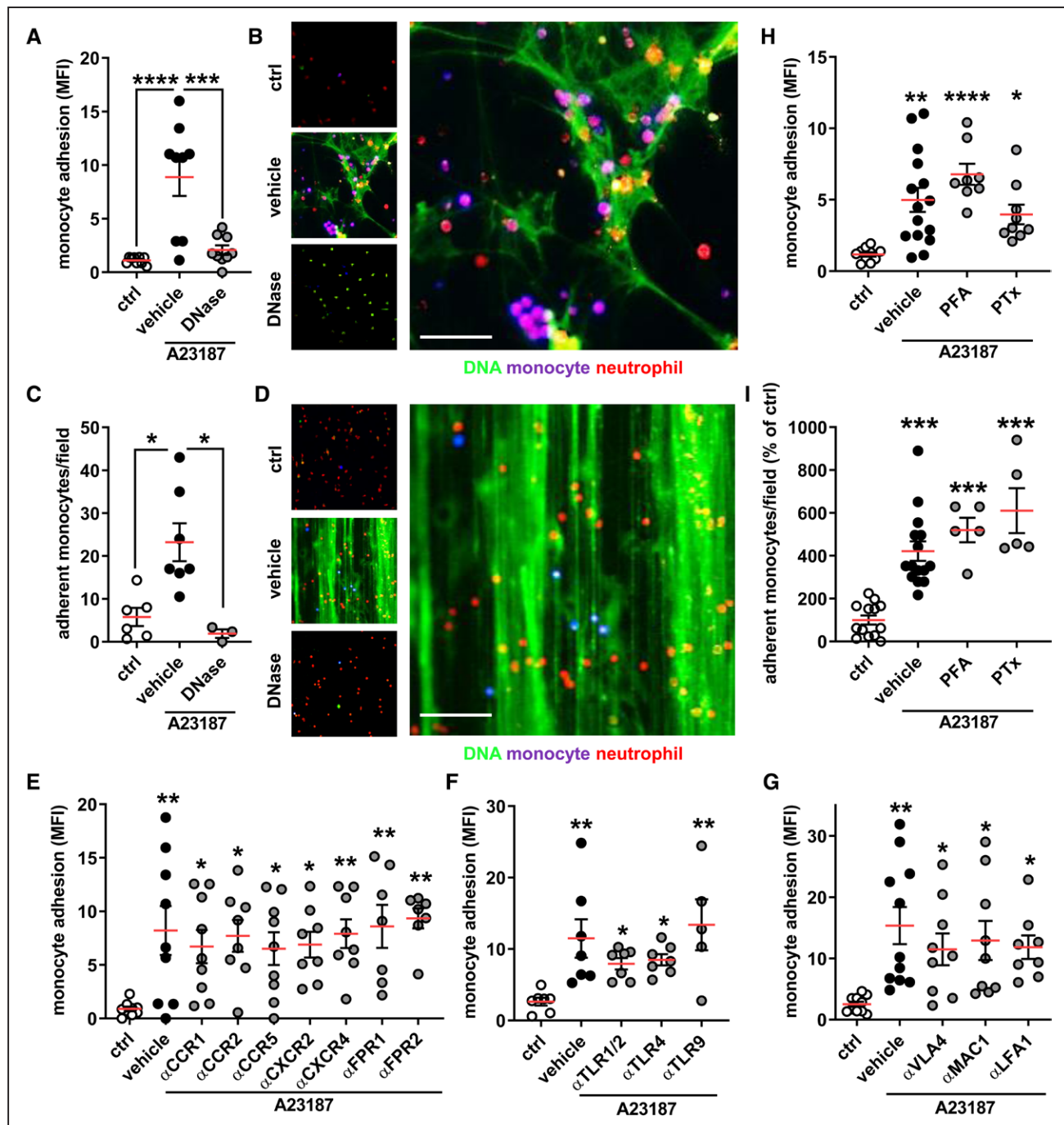


Figure 2. Monocyte adhesion to NETs is receptor independent.

In vitro monocyte adhesion to expelled NETs under static or flow conditions. **A** and **B**, Monocytes were added to neutrophils (ctrl) or NET-releasing neutrophils (induced by A23187) and adhesion was quantified by a fluorescence plate reader. NETs were also degraded by DNase I. Representative microscopic image (**B**) of monocytes (violet) adherent to NETs (green; neutrophils red), scale bar 50=μm. **C** and **D**, Monocytes were perfused at 0.5 dyne/cm² over neutrophils, NETs, or degraded NETs, and their adhesion was quantified manually. Representative microscopic image (**D**) of monocytes (violet) adherent to NETs (green; neutrophils red), scale bar=100 μm. **E** through **G**, Monocytes were pretreated with antagonists or antibodies to chemokine receptors (**E**), Toll-like receptors (**F**), or integrins (**G**) before incubation with NETs. **H** and **I**, Monocytes fixed with PFA or treated with pertussis toxin (PTx) were used in static (**H**) or flow (**I**) adhesion assays. Data are analyzed by 1-way ANOVA with Tukey multiple comparisons test (**A**, **H**, **G**) or Kruskal-Wallis test with Dunn multiple comparisons test (**C**, **E**, **F**, **I**); *P≤0.05, **P≤0.01, ***P≤0.001, ****P≤0.0001. All data are presented as mean±SEM. ctrl indicates control; MFI, mean fluorescence intensity; NET, neutrophil extracellular trap; and PFA, paraformaldehyde.

NET-Resident Histone H2a Attracts Monocytes Electrostatically

Given the signaling-independent adhesion of monocytes to NETs, we assumed that biophysical interactions

such as electrostatic charges could be important in this process. In fact, monocytes present an overall negative surface charge (ζ potential -10.51 ± 0.69 mV), whereas NETs are decorated with highly cationic proteins. To test the importance of charge interaction in the adhesion

of classical monocytes to NETs, monocytes were incubated with either cholesterol sulfate or oleylamine. Cholesterol sulfate is a negatively charged steroid lipid, whereas oleylamine is a positively charged unsaturated fatty acid. Both lipids integrate with their lipophilic part into the phospholipid bilayer of the cell membrane and hence allow manipulating cell surface charge. In our hands, incubation with cholesterol sulfate or oleylamine rendered monocyte surface charges more negative or more positive, respectively (Figure 3A and 3B). To assess the relevance of the monocyte surface charge during adhesion to NETs, we allowed human classical monocytes of different surface charges to adhere to NETs. In these experiments, we were able to generate a stringent correlation with more negative surface charges resulting in higher monocyte adhesion and vice versa (Figure 3C). To assess the physical properties of charge-dependent adhesion in more depth, we performed atomic force spectroscopy with a monocyte immobilized at the tip of the cantilever. Atomic force microscopy is a scanning probe microscope with piezoelectric elements to move the springlike cantilever. The deflecting cantilever is used to directly measure forces acting on the monocyte. A force-distance curve reports on the contact force (I), the force until maximum adhesion (II), the forces needed to fully detach the monocyte from the NET (III), and the distance of this detachment (IV) (Figure 3D). Classical monocytes with different surface charges were immobilized at the tip of the atomic force microscopy cantilever and, in this position, probed on NETs. Manipulation of the monocyte surface charges impacted the maximum adhesion force, the detachment force, and the detachment distance to separate monocytes from NETs, the energy required to separate the monocyte from the NET, and the adhesion frequency. Overall, NET-adhesion strength and the ability to adhere to NETs was heightened when monocytes were rendered more negatively charged, and opposite effects were found in less negatively charged monocytes (Figure 3E through 3I, [Figure IIIA through IIIC in the Data Supplement](#)), thus confirming the concept of charge-driven monocyte adhesion.

NETs are decorated with a large array of granule-derived, cytoplasmic, and nuclear proteins. Proteomics of NETs allowed the identification of 73 enriched polypeptides of which 2 clusters exhibited cationic surface charge as deferred from the peptides' isoelectric point. One cluster was centered on nuclear histones of which histone H2a is the most abundant. A second cluster revealed antimicrobial polypeptides with MPO and cathepsin G being the 2 candidates characterized by both cationic charge and high abundance (Figure 3J, [Table II in the Data Supplement](#)). To assess the contribution of these NET-resident proteins toward monocyte adhesion, we treated NETs with antibodies toward these polypeptides and recorded adhesion of human

classical monocytes. In these studies, neutralization of antimicrobial polypeptides abundantly found in NETs (MPO, cathepsin G) and of antimicrobial polypeptides previously found to contribute to monocyte adhesion (LL37, elastase, proteinase 3, HNP1-3) yielded no effect (Figure 3K, [Figure IIII in the Data Supplement](#)).^{4,5,23} In addition, neutralization of highly abundant S100A8/9 peptides failed to reduce monocyte adhesion ([Figure IIJJ in the Data Supplement](#)). However, neutralization of histone H2a, the most abundant nuclear protein found in NETs, fully abrogated NET-driven monocyte adhesion (Figure 3K). High-resolution confocal microscopy revealed that monocytes indeed bound to NET-resident histone H2a (Figure 3L). Last, histone H2a binds to human classical monocytes in a charge-dependent fashion (Figure 3M), thus confirming our understanding of charge-mediated monocyte adhesion. When studying the binding of histone H2a to monocyte subsets, we found that a similar percentage of both classical and nonclassical monocytes reacted with histone H2a ([Figure IIKK in the Data Supplement](#)). However, histone H2a bound in much higher intensity to classical monocytes in comparison with their nonclassical counterparts regardless whether they expressed Slan or not ([Figure IIIL in the Data Supplement](#)).

Therapeutic Neutralization of Histone H2a Diminishes Arterial Monocyte Adhesion and Atheroprogession During Endotoxemia

Thus far, our data suggest that histone H2a presented in NETs released during endotoxemia causes myeloid cell adhesion, a process dramatically accelerating atheroprogession. Hence, we devised a protocol aimed at halting histone H2a-induced monocyte adhesion in vivo. Herein, a histone H2a-neutralizing antibody or an isotype control immunoglobulin G was administered in hypercholesterolemic mice treated with LPS for 4 hours, and luminal adhesive events were studied by intravital microscopy (Figure 4A). Although treatment with histone H2a-targeting antibodies did not impact the presence of luminal NET-like structures and the number of circulating leukocytes, adhesion of myeloid cells was significantly reduced (Figure 4B through 4D, [Figure IIV and IIVB in the Data Supplement](#)). Whereas antibody targeting in vivo may be associated with undesired side effects, we aimed at generating an alternative interference strategy. A resurgence of peptides as therapeutic agents to treat many diseases, especially for cardiovascular disease, has inspired us to develop peptidic inhibitors to neutralize histone H2a. Peptides contain several advantages such as ease of synthesis and optimization to improve pharmacokinetic and binding properties, large-scale and cost-effective production, and applicability to

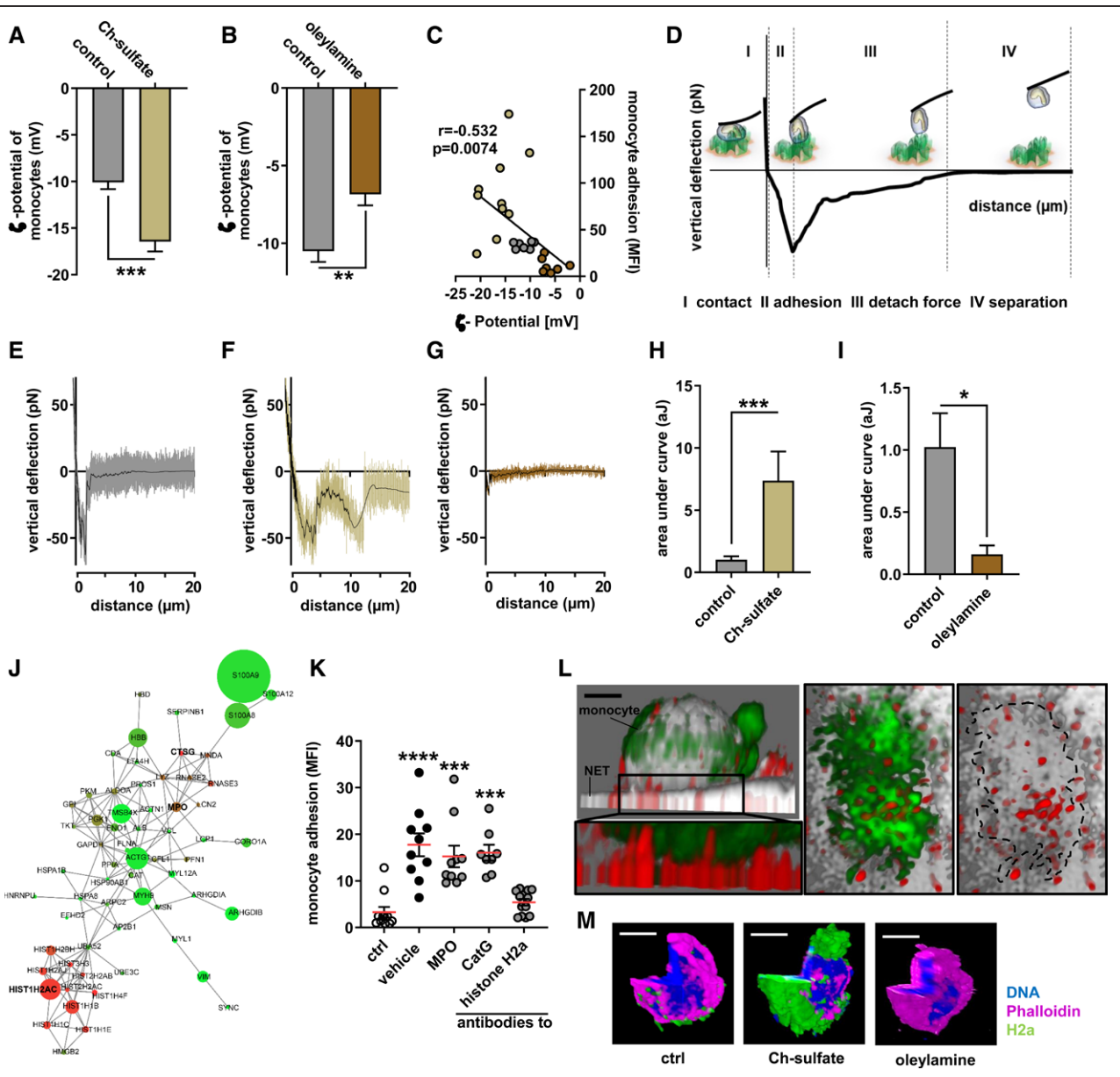


Figure 3. Monocyte adhesion to NETs is regulated by cationic histone H2a.

A and **B**, ζ -potential analysis of isolated monocytes treated with Ch-sulfate (**A**) or oleylamine (**B**). **C**, Pearson correlation of monocyte adhesion to NETs versus monocyte ζ -potential. **D**, Scheme of single-cell atomic force microscopy force spectroscopy. Monocytes were probed on expelled NETs at 200 pN contact force. **E** through **G**, Representative force curves of native monocytes (**E**) or monocytes treated with Ch-sulfate (**F**) or oleylamine (**G**) probed on NETs. **H** through **I**, Quantification of the area under the curve reflecting the energy required to rupture the monocyte-NET interaction. **J**, Proteome analysis of NET-resident proteins. Circle size reflects protein abundance, whereas color codes represent charge (red cationic, green anionic). **K**, Monocyte adhesion to NETs preincubated with antibodies to indicated NET-associated proteins. **L**, Representative immunofluorescence confocal microscopy image showing the tight interaction between NET resident histone H2a and a NET-bound monocyte, scale bar=3 μ m. Displayed is a xy projection (DNA gray, monocyte green, and histone H2a red) and a zoom-in underneath (monocyte green, histone H2a red). The right 2 images represent a top view (xz) of the zoom-in area, thus visualizing the interface between the monocyte (green) and NET-resident histone H2a (red). In the right-most image the monocyte is outlined (dashed line). **M**, Representative confocal microscopy images of histone H2a binding monocyte in a charge-dependent manner (DNA blue, monocyte purple, histone H2a green), scale bar=5 μ m. Data are analyzed by unpaired *t* test (**A**, **B**, **H**, **I**) or Kruskal-Wallis test with Dunn multiple comparisons test (**K**); * $P \leq 0.05$, ** $P \leq 0.01$, *** $P \leq 0.001$. All data are presented as mean \pm SEM. CatG indicates cathepsin G; Ch, cholesterol; ctrl, control; MFI, mean fluorescence intensity; MPO, myeloperoxidase; and NET, neutrophil extracellular trap.

conjugate with specific probes for drug delivery or for use as imaging tools.²⁴ Moreover, we have previously demonstrated and proven that monocyte adhesion can be interrupted by peptidic inhibitors,^{5,25} and the highly positively charged N-terminus of histone H4 can be neutralized by the cyclic peptide.²⁶ By use of the same

structure-based approaches as in our previous work, we in silico designed and developed peptides targeting histone H2a. A few peptide candidates were selected based on binding free energy and visual inspection of the interactions between the candidates and the N-terminal tail of histone H2a for further synthesis and functional

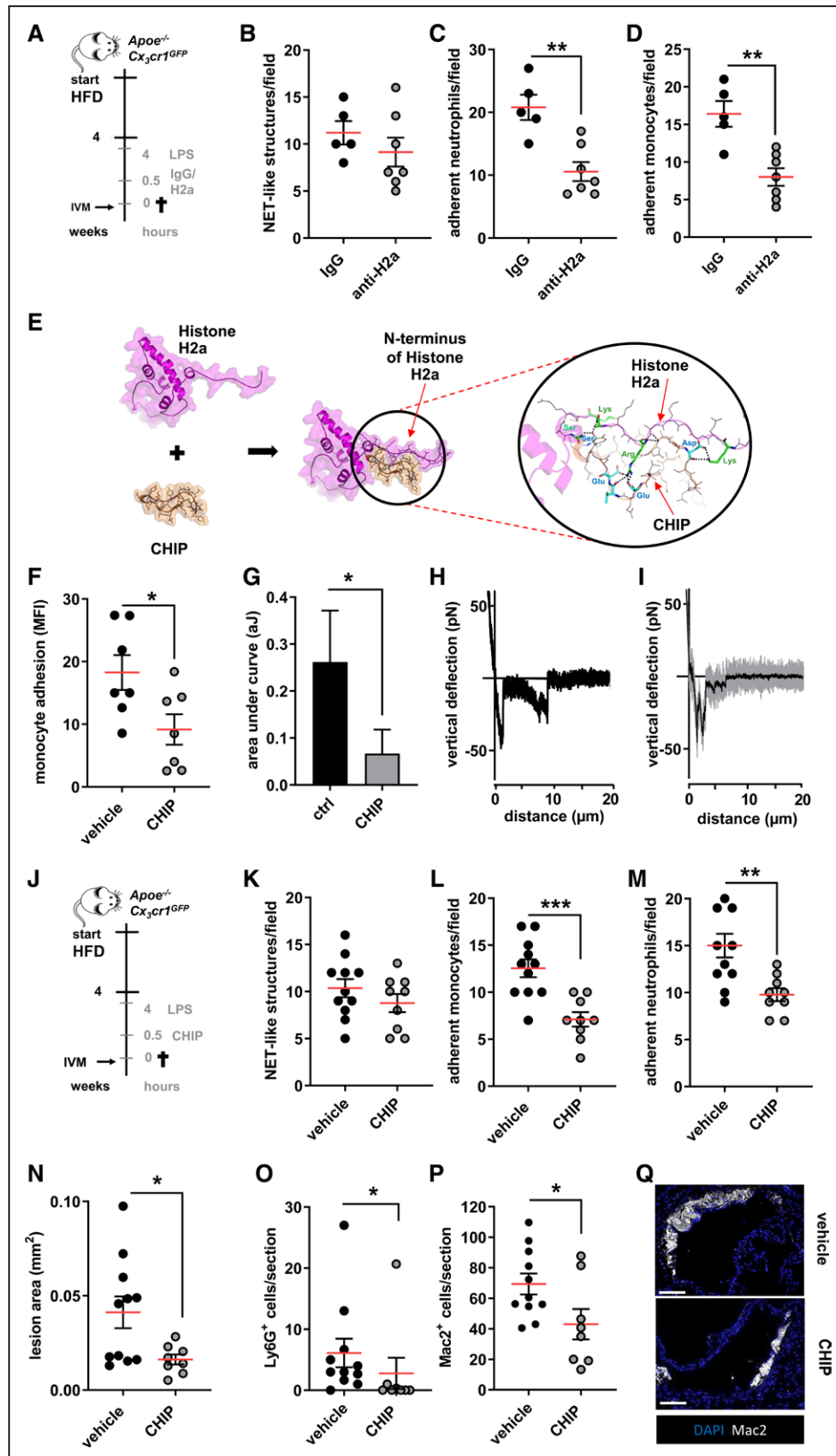


Figure 4. Neutralization of histone H2a inhibits endotoxin-induced arterial myeloid cell recruitment and atheroprotection.

A, Experimental outline. *ApoE*^{-/-} *Cx3cr1*^{GFP} were fed a HFD for 4 weeks, treated with LPS (1 mg/kg, 4 hours), and injected with isotype respective control (IgG), or a histone H2a–targeting antibody (anti-H2a). **B** through **D**, Intravital microscopy was used to quantify luminal NET-like structures (**B**) in the left carotid artery, and adherent neutrophils (**C**) and monocytes (**D**), as well. **E**, The structure of histone H2a (magenta), CHIP (orange), and the histone H2a–CHIP complex that was derived from protein–protein docking and molecular dynamic simulation. CHIP bound and interacted with the N-terminal part of histone H2a. (Continued)

Figure 4 Continued. The electrostatic interactions between Arg or Lys of histone H2a (green sticks) with Glu or Asp of CHIP (cyan sticks), and hydrogen bonds (displayed as dash lines), as well, help to stabilize the complex formation between histone H2a and CHIP. **F** through **I**, Pharmacological interruption of histone H2a monocyte binding was validated in static adhesion assays (**F**), and by single-cell force spectroscopy (**G** through **I**), as well. (**J** through **Q**, In vivo validation of the therapeutic effect of CHIP in endotoxin-accelerated atherosclerosis. **J**, Experimental outline. *Apoe*^{-/-} *Cx₃cr1*^{GFP} were fed a HFD for 4 weeks, treated with LPS (1 mg/kg, 4 hours) and injected with vehicle or CHIP (5 mg/kg). **K** through **M**, Intravital microscopy was used to quantify luminal NET-like structures (**K**) in the left carotid artery, and adherent neutrophils (**L**) and monocytes (**M**), as well. **N**, Aortic root lesion size analyzed after hematoxylin and eosin staining. Quantification of lesional neutrophils (Ly6G⁺ cells) (**O**), and macrophages (Mac2⁺ cells) (**P**). **Q**, Representative immunofluorescence images showing lesional Mac2⁺ cells (gray) and nuclei (DAPI, blue), scale bar=50 μm. Data are analyzed by the Mann-Whitney *U* test (**B** through **D**, **F**, **G**, and **O**) or unpaired *t* test (**K** through **N** and **P**); **P*≤0.05, ***P*≤0.01, ****P*≤0.001. All data are presented as mean±SEM. CHIP indicates cyclic histone 2a interference peptide; DAPI, 4',6-diamidino-2-phenylindol; HFD, high-fat diet; IgG, immunoglobulin G; IVM, intravital microscopy; LPS, lipopolysaccharide; MFI, mean fluorescence intensity; MPO, myeloperoxidase; and NET, neutrophil extracellular trap.

characterization. The most potent peptide, CHIP, bound with the N-terminal domain of histone 2A. The electrostatic interactions between positively charged residues (Arg and Lys) of histone H2a with negatively charged residues (Asp and Glu) of CHIP and H-bond interactions promoted a stable complex formation (Figure 4E). To test the functionality of this peptide, we first performed in vitro experiments. Herein, pretreatment of NETs with CHIP reduced adhesion significantly (Figure 4F). CHIP biophysically reduced the interaction strength of monocytes and NETs as shown by atomic force microscopy (Figure 4G through 4I). Given these encouraging findings, we aimed at testing CHIP in vivo. Delivery of CHIP to hypercholesterolemic mice receiving LPS for 4 hours did not impact the presence of NET-like structures in the arterial lumen, but significantly diminished arterial adhesion of neutrophils and monocytes (Figure 4J through 4M). Beyond impacting luminal events, CHIP allowed the drastic reduction of atherosclerotic lesion sizes (Figure 4O). These changes in lesion size were not associated with differences in blood counts or plasma lipid levels (Figure IV C through IV F in the Data Supplement). The lesions of mice treated with CHIP were characterized by the accumulation of fewer neutrophils and macrophages (Figure 4P through 4R). In line herewith, aortic neutrophil and monocyte numbers were strikingly reduced by CHIP (Figure IV G and IV H in the Data Supplement). Taken together, neutralization of histone H2a by antibodies or peptides allows the reduction of arterial myeloid cell recruitment and accelerated atherosclerosis evoked by endotoxemia.

DISCUSSION

Atherosclerosis is the leading cause of mortality in Western society. Excess mortality from cardiovascular disease during influenza epidemics was first recognized early in the 20th century, but the specific association of influenza and other infections with myocardial infarction was not characterized until decades later. In fact, over the past 20 years, epidemiological studies have consistently demonstrated the association between acute infection with multiple bacterial and viral pathogens and the short-term increase in cardiovascular complications.⁸ For example, a self-controlled case series involving US veterans showed a remarkable

increase in the risk of myocardial infarction during the first 15 days after hospitalization for acute bacterial pneumonia, to a risk that was 48 times higher than that in any 15-day period during the year before or after the onset of infection.²⁷ An increase in the short-term risk of myocardial infarction has also been described in association with urinary tract infection and bacteremia.^{9,10} The strength and temporal pattern of the association between acute infections and an increased risk of myocardial infarction suggest a causal relationship. Because the association has been shown with a variety of pathogens, sites of infection, and the association is stronger and lasts longer when the infection is more severe, it is likely that the infection and the host response to infection are major determinants in this relationship. Here, we used a model of endotoxemia to mimic acute, severe infection. In these experiments, administration of endotoxin induces a rapid expansion of atherosclerotic lesions characterized by extension of the lesional myeloid cell compartment. This increase was fully abrogated when release of NETs was pharmacologically inhibited. Our studies identify a mechanism that centers on monocyte adhesion to luminal NETs, in general, and to NET-resident histone H2a, in particular. Neutralization of histone H2a by antibodies or by in silico designed peptides permits inhibition of endotoxin-accelerated monocyte adhesion and lesional myeloid cell accumulation, thus providing a potential strategy for improved care of patients at risk of cardiovascular events and experiencing an acute infection.

Because our study was performed with endotoxin stimulation only, this may be perceived as a limitation in the applicability of our study to clinical scenarios. However, an increased risk for cardiovascular complications after an acute infections has been observed for numerous pathogens, including viruses such as influenza virus or respiratory syncytial virus, Gram-positive bacteria including *Streptococcus pneumoniae* and *Staphylococcus aureus*, and Gram-negative bacteria like *Escherichia coli* and *Haemophilus influenzae*, as well.^{8,10,12,28} NET release is triggered by a variety of stimuli including all of the pathogens listed earlier²⁹; hence, the NET-centered mechanism identified in our study may in part be applicable to a large variety of pathogen-associated cardiovascular complications, although confirmation in additional studies is required.

Neutrophils have previously been reported to pave the way for inflammatory monocytes into developing atherosclerotic lesions. Rendering mice neutropenic during the initial stages of atherosclerosis diminishes lesion sizes, and lesion composition, as well, with lowered macrophage accumulation.³⁰ Neutrophils stimulate various mechanisms that promote monocyte recruitment. Among these, secretion of chemotactic proteins stands out as an important mechanism for arterial monocyte recruitment. Cathepsin G, cathelicidin, complexes formed of neutrophil-derived α -defensin and platelet-borne CCL5, and CCL2 released from neutrophils in a circadian fashion were shown to induce firm monocyte adhesion in mouse models of vascular inflammation when immobilized on arterial endothelial cells.^{3–5,31} However, all these ligands bind to specific receptors and increase adhesion through increased integrin affinity and avidity. In our study, we identify electrostatic interactions between cationic histone H2a and negatively charged classical monocyte surfaces as a novel mechanism driving infection-associated monocyte recruitment into atherosclerotic lesions. Histone H2a combines abundance within NETs and surface charge and may hence stand out as an important epitope for monocyte adhesion. However, other histone isoforms may engage similar activities because they are comparable in abundance and charge within NETs. Of note, a recent study has shown that activated smooth muscle cells residing in the fibrous cap of advanced atherosclerotic lesions stimulate neutrophils to release NETs. These are rich in cytotoxic histone H4 that can puncture human and murine SMCs leading to their death and, when reoccurring, thinning of the fibrous cap.²⁶ Thus, therapeutic neutralization of histone epitopes may exert a dual beneficial effect allowing the limitation of the macrophage burden and fibrous cap thinning.^{32,33}

The mechanism of NET-driven monocyte recruitment is receptor independent and hence lacks specificity. In unpublished observations, we also found that neutrophils adhere to NETs. Consequently, continued inhibition of neutrophil adhesion to NETs may lower the number of neutrophils at sites of inflammation and thereby reduce local NET burden. In addition, surgical removal of tumors (especially colorectal cancer) is frequently associated with bacteremia, and NETs triggered in such settings have been suggested to promote immobilization of tumor cells in vascular beds, thus promoting formation of metastases.^{34–36} Mechanistically, some studies reported β 1 integrins on tumor cells to mediate adhesion to NETs, whereas other studies found unspecific binding to NETs underlying the process of NET-driven metastasis.^{2,19,20} Consequently, degradation of NETs using DNase I has been found to limit metastases formation in animal models combining infection and tumor development.^{2,19} Observations made in the present study suggest that histone H2a can also promote adhesion of

tumor cells and promote metastases, and perioperative treatment with histone-neutralizing therapies may provide an efficient way to reduce cancer spreading.

Monocyte adhesion to endothelial cells is typically looked on as a bicellular interaction.³⁷ However, such a simplified model can be modified by accessory cells including platelets and neutrophils through direct interaction or release of secretory products with chemotactic effects.^{38,39} In the context of atherogenesis, NET release along the arterial endothelium appears to be an infrequent event,¹⁴ making a major contribution of NETs as adhesive substrate for monocytes unlikely. Irrespective of this conclusion, depletion of NETs during early stages of atherosclerosis has repeatedly been shown to limit lesion size and macrophage accumulation.^{40,41} Whether reduced macrophage accumulation in these studies is a consequence of lowered monocyte adhesion and possibly processes described in this study remains to be determined. In an acute inflammatory setting, such as a LPS challenge, however, luminal NET burden increases and herewith the chance for monocytes to adhere to NETs in this location. Based on our *in vitro* experiments, it seems unlikely that histone H2a is deposited on the arterial endothelium because digestion of NETs on endothelial cells prevents monocyte adhesion. Yet another intriguing aspect of NETs in luminal location is their potential contribution to endothelial erosion. Previous reports have pointed to a mechanism by which NETs released at sites of disturbed flow contribute to endothelial cell death and subsequent endothelial denudation.^{42,43} Further studies are required to investigate if NET-resident cytotoxic components such as histones^{25,44} contribute to this process.

Although our study aims at understanding the acute effect of LPS on atherosclerosis development, others have reported the impact of chronic LPS delivery.⁴⁵ In such a setting, atherosclerotic plaques of mice receiving LPS are infiltrated by NK1.1 cells and T cells together promoting a proinflammatory microenvironment. In addition, activated lymphocytes populated the adventitia in these mice. In a similar disease model, the apolipoprotein C-I–dependent activation of macrophages was found to be crucial.⁴⁶ Thus far, however, the involvement of neutrophils in models of chronic LPS exposure in the context of atherosclerosis has not been studied. One limiting factor may be the development of neutrophilic myeloid-derived suppressor cells in the spleens of mice chronically challenged with LPS,⁴⁷ and future studies need to clarify the importance of neutrophils in such settings.

Infections in patients with cardiovascular risk increase the chance of cardiovascular complications severalfold within the first 3 weeks after an infection. We here identify a mechanism centered on extracellular histone H2a that induces adhesion and recruitment of monocytes. Although data from the CANTOS trial (Cardiovascular

Risk Reduction Study [Reduction in Recurrent Major CV Disease Events]) reveal the overall positive effects of anti-inflammation therapy in the context of atherosclerosis, neutralization of interleukin 1 β was also associated to heightened risk of bacterial infections.⁴⁸ Therapeutic neutralization of histone H2a will likely not be linked to such adverse side effects, because the antimicrobial actions of histone H2a can be compensated by the abundance of other antimicrobial polypeptides residing within NETs. In addition, the strict focus on infection-associated cardiovascular complications will be relevant to a very short time window of now >3 weeks after infection and can be combined with standard antibiotic treatment. Thus, targeting histone H2a may stand out as an innovative way to lower arterial monocyte recruitment accelerated by infection while coming with limited intrinsic side effects.

ARTICLE INFORMATION

Received March 5, 2020; accepted October 23, 2020.

The Data Supplement is available with this article at <https://www.ahajournals.org/doi/suppl/10.1161/CIRCULATIONAHA.120.046677>.

Authors

Ariane Schumski, MSc; Almudena Ortega-Gómez^{1D}, PhD; Kanin Wichapong^{1D}, PhD; Carla Winter, PhD; Patricia Lemnitzer, BSc; Joana R. Viola, PhD; Mayra Píñilla-Vera, MD; Eduardo Folco, PhD; Victor Solís-Mezarino, PhD; Moritz Völker-Albert, PhD; Sanne L. Maas, MSc; Chang Pan, MD; Laura Perez Olivares, MSc; Janine Winter, BSc; Tilman Hackeng, PhD; Mikael C.I. Karlsson, MD; Tanja Zeller, PhD; Axel Imhof, PhD; Rebecca M. Baron, MD; Gerry A.F. Nicolaes, PhD; Peter Libby^{1D}, MD; Lars Maegdefessel, MD, PhD; Frits Kamp, PhD; Martin Benoit, PhD; Yvonne Döring, PhD; Oliver Soehnlein^{1D}, MD, PhD

Correspondence

Oliver Soehnlein, MD, PhD, IPEK, LMU Munich, Pettenkoferstr. 9, 80336 Munich, Germany. Email oliver.soehnlein@gmail.com

Affiliations

Institute for Cardiovascular Prevention (IPEK), LMU Munich Hospital, Germany (A.S., A.O.-G., C.W., P. Lemnitzer, J.R.V., C.P., L.P.O., J.W., Y.D., O.S.). German Center for Cardiovascular Research (DZHK), partner site Munich Heart Alliance (MHA), Munich, Germany (A.S., A.O.-G., S.L.M., L.M., O.S.). Department of Biochemistry, CARIM, University Maastricht, The Netherlands (K.W., T.H., G.A.F.N.). Division of Pulmonary and Critical Care Medicine (M.P.-V., R.M.B.), Division of Cardiovascular Medicine (E.F., P. L.), Brigham and Women's Hospital, Harvard Medical School, Boston, MA. EpiQMAx GmbH, Planegg-Martinsried, Germany (V.S.-M., M.V.-A.). Department of Microbiology, Tumor and Cell Biology (M.C.I.K.), Department of Physiology and Pharmacology (FyFa) (O.S.), Karolinska Institute, Stockholm, Sweden. Department of General and Interventional Cardiology, University Heart Center Hamburg, Germany (T.Z.). German Center for Cardiovascular Research (DZHK), Partner Site Hamburg, Lübeck, Kiel Hamburg, Germany (T.Z.). BMC, Chromatin Proteomics Group, Department of Molecular Biology (A.I.), BMC, Metabolic Biochemistry (F.K.), LMU München, Germany. Department of Vascular and Endovascular Surgery, Technical University Munich, Germany (L.M.). Center for Nano Science (CeNS), Department of Physics, Munich, Germany (M.B.). Division of Angiology, Swiss Cardiovascular Centre, Inselspital, Bern University Hospital, University of Bern, Switzerland (Y.D.).

Acknowledgments

The authors acknowledge the other investigators who made the assembly of Registry of Critical Illness (RoCI) and Study of Epigenetics in Medicine (StEM) biorepositories possible, including M. Benson and Drs Ash, Dieffenbach, Fredenburgh, and Stergachis.

Sources of Funding

The authors receive funding from the Deutsche Forschungsgemeinschaft (SO876/11-1, SFB914 TP B8, SFB1123 TP A6, TP B5, and TP Z2, OR465/1-1), the Vetenskapsrådet (2017-01762), the Else-Kröner-Fresenius Stiftung, and the Leduq foundation. Dr Libby receives funding from the National Heart, Lung, and Blood Institute (1R01HL134892), the American Heart Association (18CSA34080399), the RRM Charitable Fund, and the Simard Fund.

Disclosures

Drs Soehnlein, Wichapong, and Nicolaes hold a patent on targeting histones in cardiovascular inflammation. Dr Libby is an unpaid consultant to, or involved in clinical trials for Amgen, AstraZeneca, Baim Institute, Beren Therapeutics, Esperion, Therapeutics, Genentech, Kancera, Kowa Pharmaceuticals, Medimmune, Merck, Novartis, Pfizer, Sanofi-Regeneron. Dr Libby is a member of scientific advisory board for Amgen, Corvidia Therapeutics, DalCor Pharmaceuticals, Kowa Pharmaceuticals, Olatec Therapeutics, Medimmune, Novartis, and XBiotech, Inc. Dr Libby's laboratory has received research funding in the last 2 years from Novartis. Dr Libby is on the Board of Directors of XBiotech, Inc. Dr Libby has a financial interest in Xbiotech, a company developing therapeutic human antibodies. Dr Libby's interests were reviewed and are managed by Brigham and Women's Hospital and Partners HealthCare in accordance with their conflict of interest policies.

Supplemental Materials

Expanded Methods
Data Supplement Figures I–IV
Data Supplement Tables I–II
References 49–51

REFERENCES

- Fayad ZA, Swirski FK, Calcagno C, Robbins CS, Mulder W, Kovacic JC. Monocyte and macrophage dynamics in the cardiovascular system: JACC Macrophage in CVD Series (Part 3). *J Am Coll Cardiol*. 2018;72:2198–2212. doi: 10.1016/j.jacc.2018.08.2150
- Park J, Wysocki RW, Amoozgar Z, Maiorino L, Fein MR, Jorns J, Schott AF, Kinugasa-Katayama Y, Lee Y, Won NH, et al. Cancer cells induce metastasis-supporting neutrophil extracellular DNA traps. *Sci Transl Med*. 2016;8:361ra138. doi: 10.1126/scitranslmed.aag1711
- Winter C, Silvestre-Roig C, Ortega-Gomez A, Lemnitzer P, Poelman H, Schumski A, Winter J, Drechsler M, de Jong R, Immler R, et al. Chronopharmacological targeting of the CCL2-CCR2 axis ameliorates atherosclerosis. *Cell Metab*. 2018;28:175–182.e5. doi: 10.1016/j.cmet.2018.05.002
- Ortega-Gomez A, Salvermoser M, Rossaint J, Pick R, Brauner J, Lemnitzer P, Tilgner J, de Jong RJ, Megens RT, Jamsbi J, Döring Y, et al. Cathepsin G controls arterial but not venular myeloid cell recruitment. *Circulation*. 2016;134:1176–1188. doi: 10.1161/CIRCULATIONAHA.116.024790
- Alard JE, Ortega-Gomez A, Wichapong K, Bongiovanni D, Horckmans M, Megens RT, Leoni G, Ferraro B, Rossaint J, Paulin N, et al. Recruitment of classical monocytes can be inhibited by disturbing heteromers of neutrophil HNP1 and platelet CCL5. *Sci Transl Med*. 2015;7:317ra196. doi: 10.1126/scitranslmed.aad5330
- Zhang J, Alcaide P, Liu L, Sun J, He A, Lusinskas FW, Shi GP. Regulation of endothelial cell adhesion molecule expression by mast cells, macrophages, and neutrophils. *PLoS One*. 2011;6:e14525. doi: 10.1371/journal.pone.0014525
- Silvestre-Roig C, Braster Q, Ortega-Gomez A, Soehnlein O. Neutrophils as regulators of cardiovascular inflammation. *Nat Rev Cardiol*. 2020;17:327–340. doi: 10.1038/s41569-019-0326-7
- Musher DM, Abers MS, Corrales-Medina VF. Acute infection and myocardial infarction. *N Engl J Med*. 2019;380:171–176. doi: 10.1056/NEJMra1808137
- Smeeth L, Thomas SL, Hall AJ, Hubbard R, Farrington P, Vallance P. Risk of myocardial infarction and stroke after acute infection or vaccination. *N Engl J Med*. 2004;351:2611–2618. doi: 10.1056/NEJMoa041747
- Dalager-Pedersen M, Søgaard M, Schønheyder HC, Nielsen H, Thomsen RW. Risk for myocardial infarction and stroke after community-acquired bacteremia: a 20-year population-based cohort study. *Circulation*. 2014;129:1387–1396. doi: 10.1161/CIRCULATIONAHA.113.006699
- Ramirez J, Aliberti S, Mirsaedi M, Peyrani P, Filardo G, Amir A, Moffett B, Gordon J, Blasi F, Bordon J. Acute myocardial infarction in

- hospitalized patients with community-acquired pneumonia. *Clin Infect Dis*. 2008;47:182–187. doi: 10.1086/589246
12. Corrales-Medina VF, Alvarez KN, Weissfeld LA, Angus DC, Chirinos JA, Chang CC, Newman A, Loehr L, Folsom AR, Elkind MS, et al. Association between hospitalization for pneumonia and subsequent risk of cardiovascular disease. *JAMA*. 2015;313:264–274. doi: 10.1001/jama.2014.18229
 13. Pieterse R, Rother N, Yanginlar C, Hilbrands LB, van der Vlag J. Neutrophils discriminate between lipopolysaccharides of different bacterial sources and selectively release neutrophil extracellular traps. *Front Immunol*. 2016;7:484. doi: 10.3389/fimmu.2016.00484
 14. Megens RT, Vijayan S, Lievens D, Döring Y, van Zandvoort MA, Grommes J, Weber C, Soehnlein O. Presence of luminal neutrophil extracellular traps in atherosclerosis. *Thromb Haemost*. 2012;107:597–598. doi: 10.1160/TH11-09-0650
 15. Reyes M, Filbin MR, Bhattacharyya RP, Billman K, Eisenhaure T, Hung DT, Levy BD, Baron RM, Blainey PC, Goldberg MB, et al. An immune-cell signature of bacterial sepsis. *Nat Med*. 2020; 6:333–340. doi: 10.1038/s41591-020-0752-4
 16. Clark SR, Ma AC, Tavener SA, McDonald B, Goodarzi Z, Kelly MM, Patel KD, Chakrabarti S, McAvoy E, Sinclair GD, et al. Platelet TLR4 activates neutrophil extracellular traps to ensnare bacteria in septic blood. *Nat Med*. 2007;13:463–469. doi: 10.1038/nm1565
 17. Soehnlein O, Drechsler M, Döring Y, Lievens D, Hartwig H, Kemmerich K, Ortega-Gómez A, Mandl M, Vijayan S, Projahn D, et al. Distinct functions of chemokine receptor axes in the atherogenic mobilization and recruitment of classical monocytes. *EMBO Mol Med*. 2013;5:471–481. doi: 10.1002/emmm.201201717
 18. Swirski FK, Libby P, Aikawa E, Alcaide P, Luscinskas FW, Weissleder R, Pittet MJ. Ly-6Chi monocytes dominate hypercholesterolemia-associated monocytes and give rise to macrophages in atheromata. *J Clin Invest*. 2007;117:195–205. doi: 10.1172/JCI29950
 19. Cools-Lartigue J, Spicer J, McDonald B, Gowing S, Chow S, Giannias B, Bourdeau F, Kubes P, Ferri L. Neutrophil extracellular traps sequester circulating tumor cells and promote metastasis. *J Clin Invest*. 2013;123:3446–3458. doi: 10.1172/JCI67484
 20. Najmeh S, Cools-Lartigue J, Rayes RF, Gowing S, Vourzoumis P, Bourdeau F, Giannias B, Berube J, Rousseau S, Ferri LE, et al. Neutrophil extracellular traps sequester circulating tumor cells via β 1-integrin mediated interactions. *Int J Cancer*. 2017;140:2321–2330. doi: 10.1002/ijc.30635
 21. Monti M, De Rosa V, Iommelli F, Carriero MV, Terlizzi C, Camerlingo R, Belli S, Fonti R, Di Minno G, Del Vecchio S. Neutrophil extracellular traps as an adhesion substrate for different tumor cells expressing RGD-binding integrins. *Int J Mol Sci*. 2018;19:2350. doi: 10.3390/ijms19082350
 22. Monti M, Iommelli F, De Rosa V, Carriero MV, Miceli R, Camerlingo R, Di Minno G, Del Vecchio S. Integrin-dependent cell adhesion to neutrophil extracellular traps through engagement of fibronectin in neutrophil-like cells. *PLoS One*. 2017;12:e0171362. doi: 10.1371/journal.pone.0171362
 23. Wantha S, Alard JE, Megens RT, van der Does AM, Döring Y, Drechsler M, Pham CT, Wang MW, Wang JM, Gallo RL, et al. Neutrophil-derived cathelicidin promotes adhesion of classical monocytes. *Circ Res*. 2013;112:792–801. doi: 10.1161/CIRCRESAHA.112.300666
 24. Henninot A, Collins JC, Nuss JM. The current state of peptide drug discovery: back to the future? *J Med Chem*. 2018;61:1382–1414. doi: 10.1021/acs.jmedchem.7b00318
 25. Wichapong K, Alard JE, Ortega-Gomez A, Weber C, Hackeng TM, Soehnlein O, Nicolaes GA. Structure-based design of peptidic inhibitors of the interaction between CC chemokine ligand 5 (CCL5) and human neutrophil peptides 1 (HNP1). *J Med Chem*. 2016;59:4289–4301. doi: 10.1021/acs.jmedchem.5b01952
 26. Silvestre-Roig C, Braster Q, Wichapong K, Lee EY, Teulon JM, Berrebeh N, Winter J, Adrover JM, Santos GS, Froese A, et al. Externalized histone H4 orchestrates chronic inflammation by inducing lytic cell death. *Nature*. 2019;569:236–240. doi: 10.1038/s41586-019-1167-6
 27. Corrales-Medina VF, Serpa J, Rueda AM, Giordano TP, Bozkurt B, Madjid M, Tweardy D, Musher DM. Acute bacterial pneumonia is associated with the occurrence of acute coronary syndromes. *Medicine (Baltimore)*. 2009;88:154–159. doi: 10.1097/MD.0b013e3181a692f0
 28. Violi F, Cangemi R, Falcone M, Taliani G, Pieralli F, Vannucchi V, Nozzoli C, Venditti M, Chirinos JA, Corrales-Medina VF; SIXTUS (Thrombosis-Related Extrapulmonary Outcomes in Pneumonia) Study Group. Cardiovascular complications and short-term mortality risk in community-acquired pneumonia. *Clin Infect Dis*. 2017;64:1486–1493. doi: 10.1093/cid/cix164
 29. Delgado-Rizo V, Martínez-Guzmán MA, Iñiguez-Gutierrez L, García-Orozco A, Alvarado-Navarro A, Fafutis-Morris M. Neutrophil extracellular traps and its implications in inflammation: an overview. *Front Immunol*. 2017;8:81. doi: 10.3389/fimmu.2017.00081
 30. Drechsler M, Megens RT, van Zandvoort M, Weber C, Soehnlein O. Hyperlipidemia-triggered neutrophilia promotes early atherosclerosis. *Circulation*. 2010;122:1837–1845. doi: 10.1161/CIRCULATIONAHA.110.961714
 31. Döring Y, Drechsler M, Wantha S, Kemmerich K, Lievens D, Vijayan S, Gallo RL, Weber C, Soehnlein O. Lack of neutrophil-derived CRAMP reduces atherosclerosis in mice. *Circ Res*. 2012;110:1052–1056. doi: 10.1161/CIRCRESAHA.112.265868
 32. Döring Y, Libby P, Soehnlein O. Neutrophil extracellular traps participate in cardiovascular diseases: recent experimental and clinical insights. *Circ Res*. 2020;126:1228–1241. doi: 10.1161/CIRCRESAHA.120.315931
 33. Van Avondt K, Maegdefessel L, Soehnlein O. Therapeutic targeting of neutrophil extracellular traps in atherogenic inflammation. *Thromb Haemost*. 2019;119:542–552. doi: 10.1055/s-0039-1678664
 34. Yang LY, Luo Q, Lu L, Zhu WW, Sun HT, Wei R, Lin ZF, Wang XY, Wang CQ, Lu M, et al. Increased neutrophil extracellular traps promote metastasis potential of hepatocellular carcinoma via provoking tumorous inflammatory response. *J Hematol Oncol*. 2020;13:3. doi: 10.1186/s13045-019-0836-0
 35. Tohme S, Yazdani HO, Al-Khafaji AB, Chidi AP, Loughran P, Mowen K, Wang Y, Simmons RL, Huang H, Tsung A. Neutrophil extracellular traps promote the development and progression of liver metastases after surgical stress. *Cancer Res*. 2016;76:1367–1380. doi: 10.1158/0008-5472.CAN-15-1591
 36. Sawabata N, Okumura M, Utsumi T, Inoue M, Shiono H, Minami M, Nishida T, Sawa Y. Circulating tumor cells in peripheral blood caused by surgical manipulation of non-small-cell lung cancer: pilot study using an immunocytology method. *Gen Thorac Cardiovasc Surg*. 2007; 55:189–192. doi: 10.1007/s11748-007-0101-2
 37. Gerhardt T, Ley K. Monocyte trafficking across the vessel wall. *Cardiovasc Res*. 2015;107:321–330. doi: 10.1093/cvr/cvv147
 38. Rossaint J, Margraf A, Zarbock A. Role of platelets in leukocyte recruitment and resolution of inflammation. *Front Immunol*. 2018;9:2712. doi: 10.3389/fimmu.2018.02712
 39. Soehnlein O, Lindbom L, Weber C. Mechanisms underlying neutrophil-mediated monocyte recruitment. *Blood*. 2009;114:4613–4623. doi: 10.1182/blood-2009-06-221630
 40. Liu Y, Carmona-Rivera C, Moore E, Seto NL, Knight JS, Pryor M, Yang ZH, Hemmers S, Remaley AT, Mowen KA, et al. Myeloid-specific deletion of peptidylarginine deiminase 4 mitigates atherosclerosis. *Front Immunol*. 2018;9:1680. doi: 10.3389/fimmu.2018.01680
 41. Knight JS, Luo W, O'Dell AA, Yalavarthi S, Zhao W, Subramanian V, Guo C, Grenn RC, Thompson PR, Eitzman DT, et al. Peptidylarginine deiminase inhibition reduces vascular damage and modulates innate immune responses in murine models of atherosclerosis. *Circ Res*. 2014;114:947–956. doi: 10.1161/CIRCRESAHA.114.303312
 42. Franck G, Mawson TL, Folco EJ, Molinaro R, Ruvkun V, Engelbertsen D, Liu X, Tesmenitsky Y, Shvartz E, Sukhova GK, et al. Roles of PAD4 and NETosis in experimental atherosclerosis and arterial injury: implications for superficial erosion. *Circ Res*. 2018;123:33–42. doi: 10.1161/CIRCRESAHA.117.312494
 43. Franck G, Mawson T, Sausen G, Salinas M, Masson GS, Cole A, Beltrami-Moreira M, Chatzizisis Y, Quillard T, Tesmenitsky Y, et al. Flow perturbation mediates neutrophil recruitment and potentiates endothelial injury via TLR2 in mice: implications for superficial erosion. *Circ Res*. 2017;121:31–42. doi: 10.1161/CIRCRESAHA.117.310694
 44. Wildhagen KC, García de Frutos P, Reutelingsperger CP, Schrijver R, Aresté C, Ortega-Gómez A, Deckers NM, Hemker HC, Soehnlein O, Nicolaes GA. Nonanticoagulant heparin prevents histone-mediated cytotoxicity *in vitro* and improves survival in sepsis. *Blood*. 2014;123:1098–1101. doi: 10.1182/blood-2013-07-514984
 45. Ostos MA, Recalde D, Zakin MM, Scott-Algara D. Implication of natural killer T cells in atherosclerosis development during a LPS-induced chronic inflammation. *FEBS Lett*. 2002;519:23–29. doi: 10.1016/s0014-5793(02)02692-3
 46. Westerterp M, Berbée JF, Pires NM, van Mierlo GJ, Kleemann R, Romijn JA, Haverkes LM, Rensen PC. Apolipoprotein C-I is crucially involved in lipopolysaccharide-induced atherosclerosis development in apolipoprotein E-knockout mice. *Circulation*. 2007;116:2173–2181. doi: 10.1161/CIRCULATIONAHA.107.693382
 47. Greifenberg V, Ribechini E, Rössner S, Lutz MB. Myeloid-derived suppressor cell activation by combined LPS and IFN-gamma treatment impairs DC development. *Eur J Immunol*. 2009;39:2865–2876. doi: 10.1002/eji.200939486

-
48. Ridker PM, Everett BM, Thuren T, MacFadyen JG, Chang WH, Ballantyne C, Fonseca F, Nicolau J, Koenig W, Anker SD, et al; CANTOS Trial Group. Antiinflammatory therapy with canakinumab for atherosclerotic disease. *N Engl J Med*. 2017;377:1119–1131. doi: 10.1056/NEJMoa1707914
 49. Maruchi Y, Tsuda M, Mori H, Takenaka N, Gocho T, Huq MA, Takeyama N. Plasma myeloperoxidase-conjugated DNA level predicts outcomes and organ dysfunction in patients with septic shock. *Crit Care*. 2018;22:176. doi: 10.1186/s13054-018-2109-7
 50. Wichapong K, Poelman H, Ercig B, Hrdinova J, Liu X, Lutgens E, Nicolaes GA. Rational modulator design by exploitation of protein-protein complex structures. *Future Med Chem*. 2019;11:1015–1033. doi: 10.4155/fmc-2018-0433
 51. van Zundert GCP, Rodrigues JPGLM, Trellet M, Schmitz C, Kastiris PL, Karaca E, Melquiond ASJ, van Dijk M, de Vries SJ, Bonvin AMJJ. The HADDOCK2.2 web server: user-friendly integrative modeling of biomolecular complexes. *J Mol Biol*. 2016;428:720–725. doi: 10.1016/j.jmb.2015.09.014